A MEASUREMENT OF THE N-P TOTAL CROSS SECTION BETWEEN THE ENERGIES OF 25 AND 45 MEV

by A.K. McIlwain

August, 1971

A Thesis Submitted to
the Faculty of Graduate Studies
University of Manitoba

In Partial Fulfillment
of the Requirements for the Degree
Master of Science

Abstract

The neutron - proton total cross section has been measured with 1.5% precision between the energies of 25 and 45 MeV. Results are compared to other high precision measurements between 20 and 50 MeV.

Acknowledgements

I wish to thank the people who have helped in performing this experiment and in designing it. They include I.F. Bubb, S.N. Bunker, M. Jain, M. de Jong, J.W. Leonard, K.G. Standing and B.G. Whitmore. Thanks is also expressed to R. Danyluk for providing the PDP-9 computer programme.

TABLE OF CONTENTS

1.1 Introduction

2.1 Description of the Experiment

2.2 Experimental Layout

2.3 Experimental Procedure

3.1 Calculation of Cross Sections

3.2 Determination of Errors

3.3 Determination of the Attenuation and its Statistical Uncertainty

3.4 Internal Consistency

3.5 Energy Determination

4.1 Experimental Results

References

Appendix A

Appendix B

Appendix C

FIGURES AND TABLES

Figure (1) Schematic of Physical Layout

Figure (2) Drawing of the Neutron Collimator

Figure (3) Plot of Beam Profile

Figure (4) Electronics Diagram

Figure (5) Sample Time of Flight Spectrum

Figure (6) Relative Positions of γ and n Pulses

Figure (7) Plot of Data

Table I Sizes of Error Terms

Table II Complete List of Unnormalized Data

Table III Table of Final Results

1.1 INTRODUCTION

There have been two main reasons for the recent interest in the neutron-proton total cross section. A paper was published by G. Hreuss and T. Czibok in 1969 (1) that predicted the cross section would vary with energy in an oscillatory manner. In already-existing data, they showed evidence for a conceivable oscillation of about 50 to 70 millibarn which is about 5% of the total cross section. If these oscillations had existed, they would have thrown doubt on the shape independent effective range theory (2). As a result of this paper, various laboratories proceeded to measure the cross section to high accuracy and the laboratory at Karlsruhe shortly afterwards published a set of measurements in the range of 0.7 to 32 MeV, with accuracy of better than two percent (3). Their calculations and data showed that the probability of the existance of such oscillations was very low.

The second source of interest was a phase shift analysis by M.H. MacGregor et al (4) in 1969. Total cross sections calculated from the phase shifts can be compared to measured values. At the time these phase shifts were published, the best data available were from Harwell (5). However, the uncertainty in the measurements was quite large (about ±5%) and it would be interesting to see how well some high precision data would fit the calculated cross sections. According to results published by Brady et al. at U.C. Davis (6) the calculated cross section is somewhat lower than the measured value. If there is in fact a fairly large discrepancy, the MacGregor phase shifts should be checked with the more accurate cross section data in mind. This was another reason for making the cross section measurements.

At the time of this experiment, the need was felt to remeasure the total cross section at accuracies of 1% or better. The energy range available at the University of Manitoba was especially useful as it overlapped the Canberra (7) and Karlsruhe results at the lower end and extended well up into the range measured at U.C. Davis. Since these were the only results available with quoted high accuracy, it was considered useful to reproduce the measurements and fill in gaps between. Then a comparison could be drawn between our data and the other existing data.

2.1 DESCRIPTION OF THE EXPERIMENT

The experiment was performed by making a transmission measurement of neutrons through a hydrocarbon absorber. This was compared with the transmission through a carbon absorber with a density of carbon atoms per square centimeter within 2% of that of the hydrocarbon.

The neutrons were produced by the reaction $^7Li(p,n)^7Be$. This is a strongly forward peaked reaction and about 60% of the neutrons fall in a peak about 1.8 MeV wide, giving a nearly monokinetic neutron beam. The neutron energy was determined by time of flight, the time of neutron arrival at the detector being compared with that of a "prompt" gamma ray created at the target within the same 1.5 nsec. beam pulse.

The hydrocarbon absorber used in this experiment was toluene. Since a liquid helium cooled cell was available, calculations were made for use of liquid methane, hydrogen sulphide, phosphorous trihydride, and several other substances with large amounts of hydrogen. Also, pure liquid hydrogen was considered. However, the need to rapidly cycle absorbers (see page 19 for details) made the use of cooled absorbers difficult. Solid hydrocarbons such as paraffin wax and polyethylene were considered. Although pure paraffin was available, it is hard to form into a homogeneous absorber. Unfortunately, pure polyethylene $(CH_2)_n$ was hard to locate. Hence liquid toluene was used since it is a pure liquid hydrocarbon and was readily available in a spectroscopically pure sample. It was contained in a stainless steel cylinder and plates from the same stock were mounted over the carbon absorber to compensate for the ends of the cylinder.

The details of the experiment follow.

Figure (1)

SCHEMATIC OF PHYSICAL LAYOUT

This diagram shows the relative positions of the various parts of the system as described in 2.2. In fact, the monitor was located at right angles to the plane of the paper directly above the collimator, at about the angle shown.

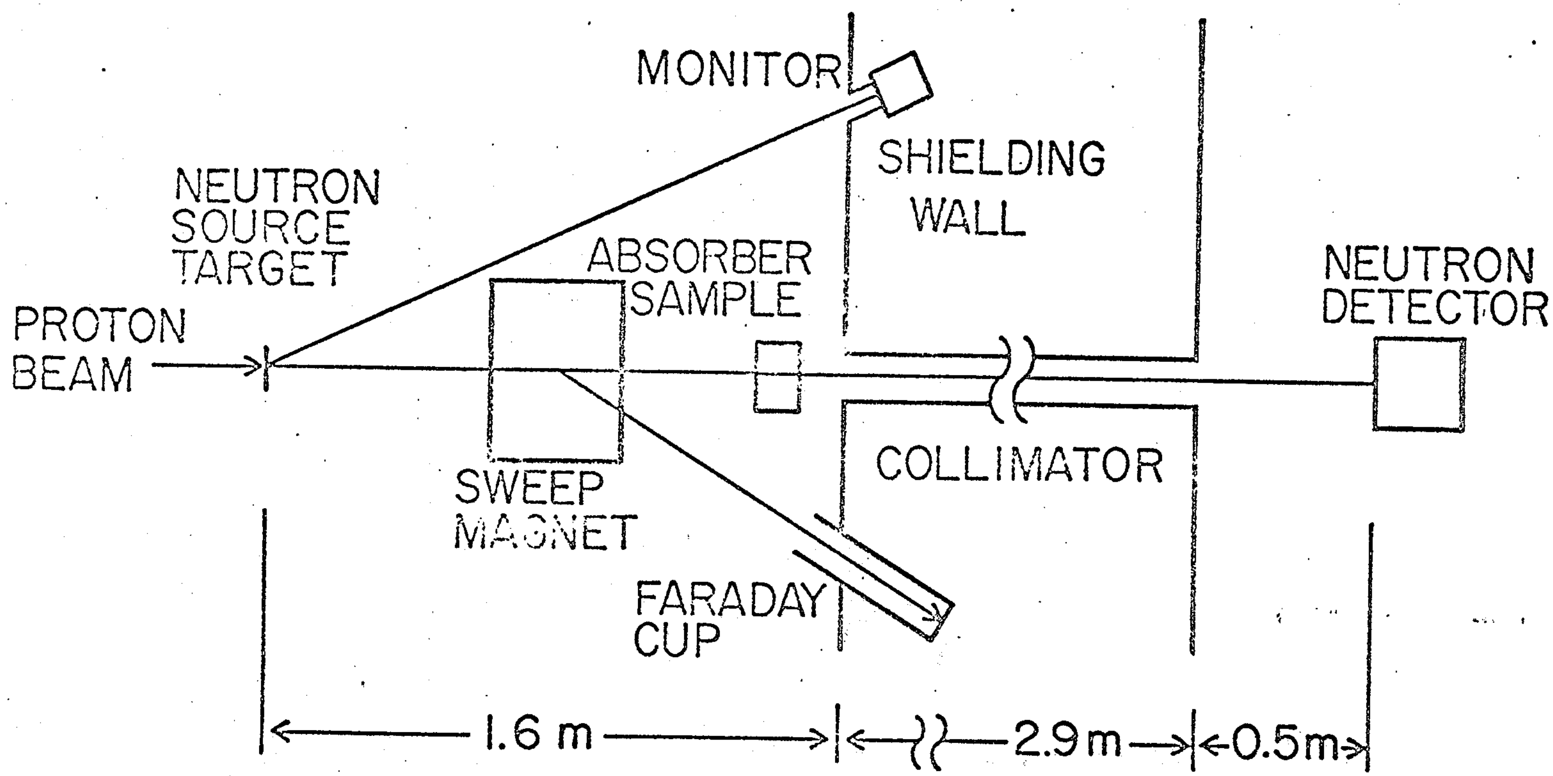
MONITOR
SHIELDING WALL
NEUTRON SOURCE TARGET
ABSORBER SAMPLE
NEUTRON DETECTOR
PROTON BEAM
COLLIMATOR
SWEEP MAGNET
FARADAY CUP
1.6 m
2.9 m
0.5 m

Fig. 1

Figure (2)

DRAWING OF THE NEUTRON COLLIMATOR

This is a scale drawing of the collimator inserted in the vault wall, (Scale 1:8). The total length of the collimator is 3.0 metres. Between the end of the steel collimator and the exit at the right there are seven equally spaced steel slugs. These are about 10 cm. thick. Complete dimensions are given in section 2.2.

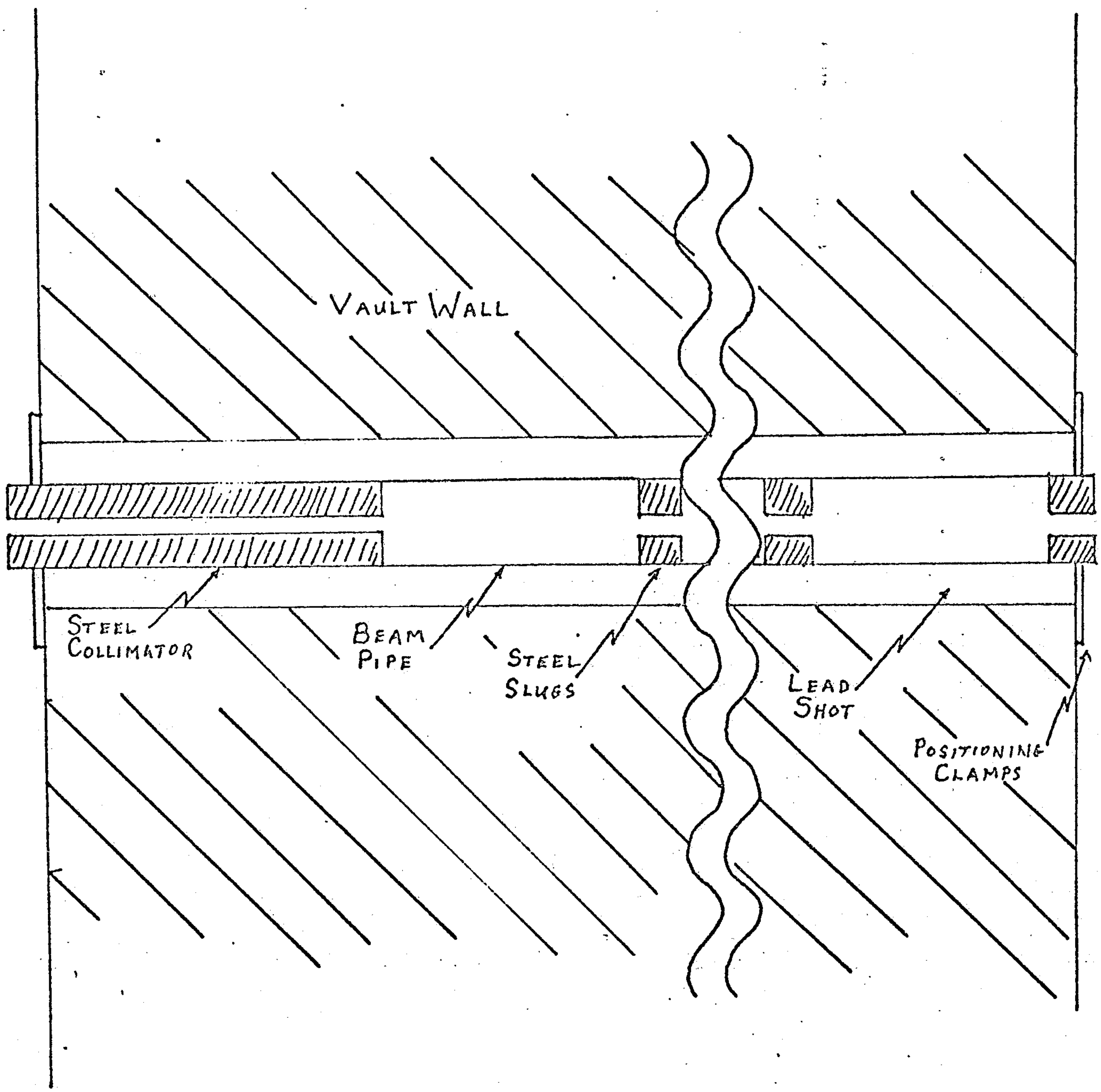

Neutron Beam Collimator

Fig. 2

2.2 EXPERIMENTAL LAYOUT

Protons produced from the sector-focused cyclotron were focused undeflected through the bending magnet onto the neutron-producing target (figure 1). A carbon collimator with a 1.3 cm. diameter aperture ensured that the proton beam would not be trimmed by the pole tips of the deflecting magnet downstream. Protons passing the collimator struck a two millimeter thick natural lithium target where the neutrons were produced. The protons were then deflected into a Faraday cup buried in the wall of the cyclotron vault.

The neutrons at zero degrees passed through the vacuum chamber of the magnet and flew in air to the detector in the experimental area. At the exit from the sweep magnet, the neutrons passed through a 1.3 cm. aluminium plate. This was used to cut down the very low energy radiation that came down the beam pipe from the cyclotron itself, and was also used to protect the photomultiplier against accidental proton bombardment. Between the magnet and the detector, the neutrons passed first through the absorbers and then through a neutron collimator placed in the vault wall. This is shown in figure 2. The collimator had a 46 cm. steel cylinder with a 1.9 cm. diameter aperture followed by seven steel slugs 10 cm. thick with 2.5 cm. diameter apertures. These were distributed uniformly over the remaining 2.4 meters. The steel was mounted in an aluminium beam pipe which passed through the vault wall and was surrounded by lead shot out to the 25 cm. diameter of the hole. Total calculated attenuation of the collimator through the steel was better than 10^4 for 40 MeV neutrons. This attenuation was checked with neutron beam profile measurements taken at the exit of the collimator (figure 3). The contribution to the main neutron flux at the detector from neutrons passing through the steel of the collimator was less than 0.1% for conditions in this experiment.

The detector which was situated five meters from the lithium target consisted of a NE218 liquid scintillator optically coupled to an RCA 8575 photomultiplier.

Figure (3)

PLOT OF BEAM PROFILE

This profile is shown on a semi-log scale. On the x-axis is detector position measured from beam centre and on the y-axis is log of neutron flux. Measurements were taken with a 6.5 mm. wide by 7.5 cm. high by 7.5 cm. deep NE102 plastic scintillator placed narrow edge into the beam. This coupled to an RCA 4518 photomultiplier was moved across the exit of the collimator at a distance of 500 cm. from the neutron-producing target. The width of the scintillator has not been unfolded from this spectrum.

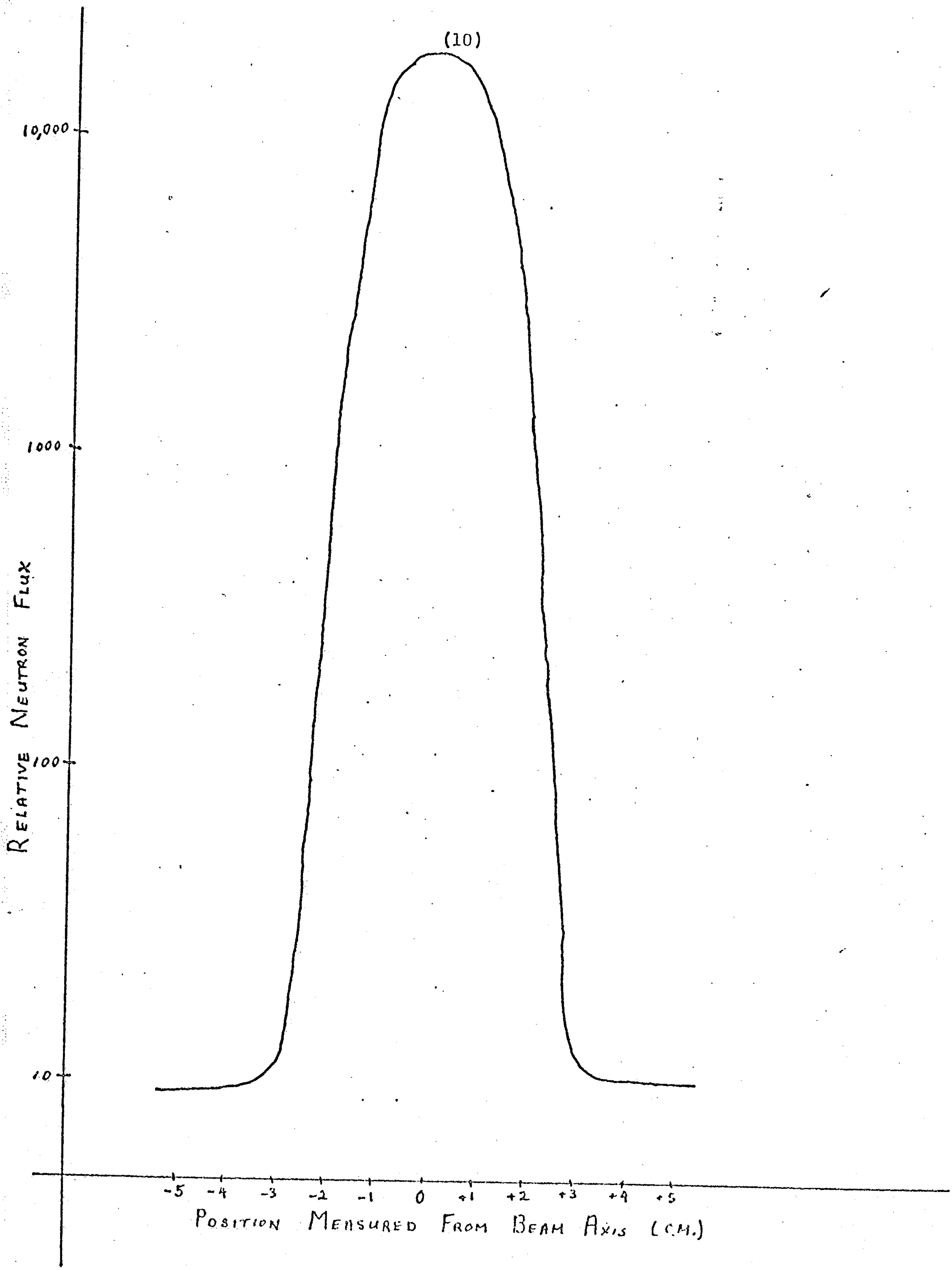
(10)
10,000
1000
100
10
Relative Neutron Flux
-5
-4
-3
-2
-1
0
+1
+2
+3
+4
+5
Position Measured From Beam Axis (C.M.)

Fig. 3

The active size of the scintillator was 5 cm. in diameter by 5 cm. thick, and the scintillator material was contained in an aluminium can about 2 mm. thick. The base of the photomultiplier contained a unity gain dynode amplifier to provide a low impedance output of the signal from dynode nine of the tube. The RCA 8575 is a high gain twelve dynode tube designed for fast timing and its anode pulse rise time is 2.1 nsec. at 3 K.V. on the anode. Since a linear signal was required from dynode nine, the tube was biased at 2250 V. on the anode. This prevented saturation at dynode nine, but still allowed a fast saturating timing pulse to be formed at the anode for all but the lowest energy gamma rays.

In the wall of the vault at about 30 degrees above the neutron collimator was situated a second detector called the monitor. This was the same as the first detector but was shielded from vault radiation and opened only in the direction of the lithium target. It was used to monitor the neutron flux for normalization purposes, and only the dynode signal from this tube was used.

As mentioned earlier, a time of flight system was used in this experiment (figure 4). The time to amplitude converter (TAC) used for the timing in this experiment received start pulses from the anode of the detector. The anode pulses were clipped with 28 cm. of 50 ohm cable shorted at the end. These triggered a zero crossing discriminator that provided start pulses. Stop pulses came from the cyclotron r.f.. This means that time intervals were measured starting from a detector pulse and ending with a pulse derived from the cyclotron r.f. Since the events of interest were synchronized to the r.f. through the beam pulses arriving at the lithium target, peaks were formed at particular places in the time spectrum corresponding either to neutrons arriving at the detector in a nearly monochromatic neutron beam or prompt gamma bursts from the lithium. This system would produce a single neutron and gamma peak. For the purpose of time calibration and energy determination, it was convenient to have a double spectrum in time with a second neutron and gamma peak. This was accomplished by stopping the TAC every other r.f. period. A typical spectrum is shown in figure 5. A more detailed explanation of the interpretation of the spectrum for energy determination is given in section 3.5 (page 28).

The spectrum produced in the above manner has a background of random gammas and low energy neutrons. If ratios of peak areas are to give correct cross sections the background must be removed. This is done electronically by setting an amplitude threshold on the dynode signal. This was effective since the gamma rays and low energy neutrons produce pulses of lower amplitude than the high energy neutrons in the peaks. This amplitude discriminator gated the time of flight system.

The gated TAC output was analysed into 1024 channels by a Northern Scientific ADC which was connected to the PDP-9 computer. This stored the data on DEC-TAPE for future energy analysis. To integrate the neutron peaks for cross section determination, a single channel analyser was used to put a window around each neutron peak in the time spectrum. The output pulses from the two single channel analysers were combined by a logic "or" gate whose output was counted by a scaler.

As well as this basic arrangement, there were some additional circuits required to obtain accurate cross sections. These are described as follows:

1) For the purpose of normalizing the number of neutrons in the peaks, some monitoring of the beam current was required. This was obtained in two ways.

The monitor detector already described as being in the cyclotron vault had a threshold set on its dynode signal, just as the main detector had. The pulses over this threshold corresponded to high energy neutrons and thus the number of pulses in a given period was proportional to the neutron flux out of the lithium. There was also a conventional Faraday cup integrator used to measure the proton beam, and its input was also recorded on a scaler.

2) The time to amplitude converter was not able to accept pulses from the detector for about two microseconds while it was measuring time and delivering its output pulse. The fraction of pulses lost during this time had to be measured so that the normalized number of neutrons could be corrected. This became important where the number of pulses per second from the detector changed greatly between one absorber and the next, since a different fraction of the pulses would have been lost. Scalers to count the start pulses and the TAC gate output provided this information.

3) It was desirable to have a check on the gain stability of our photomultipliers during the experiment, since changes in gain would have changed the threshold and hence the number of pulses in the peaks. The number of pulses over the threshold was counted for each photomultiplier. Then a second higher threshold was set and again the number of pulses was recorded. Any change in gain of a tube would have shown itself as a change in the ratio of the number of pulses over the low threshold to the number of pulses over the high threshold.

4) Finally, since a prompt gamma flash was needed for energy determination, the high pulse height threshold that removed all gamma pulses was gated off during the time that the prompt gamma rays were arriving. This provided a prompt gamma peak in the spectrum. In order to do this, windows were put around the

gamma peaks in the original time spectrum without the threshold. These pulses were then put through a logic "or" into the linear gate with the threshold pulses. The full details of the electronic circuit are seen most easily from the diagram in figure (4).

All of these scalers were gated on and off together by the PDP-9 computer.

Figure (4)

ELECTRONICS DIAGRAM

The details of operation of this system are given in the text. The only further comments are that the first discriminator on the clipped anode line is a zero crossing discriminator, and that the output from the ADC goes to the PDP-9 computer. This gates all scalers on and off together. The scalers labelled 1 - 6 record the following data:

1) The number of pulses over the high dynode threshold.
2) The number of pulses over the low dynode threshold.
3) The number of start pulses arriving at the TAC.
4) The number of pulses analysed by the TAC.
5) The number of neutron pulses in the two peaks.
6) The number of pulses at the input to the ADC.

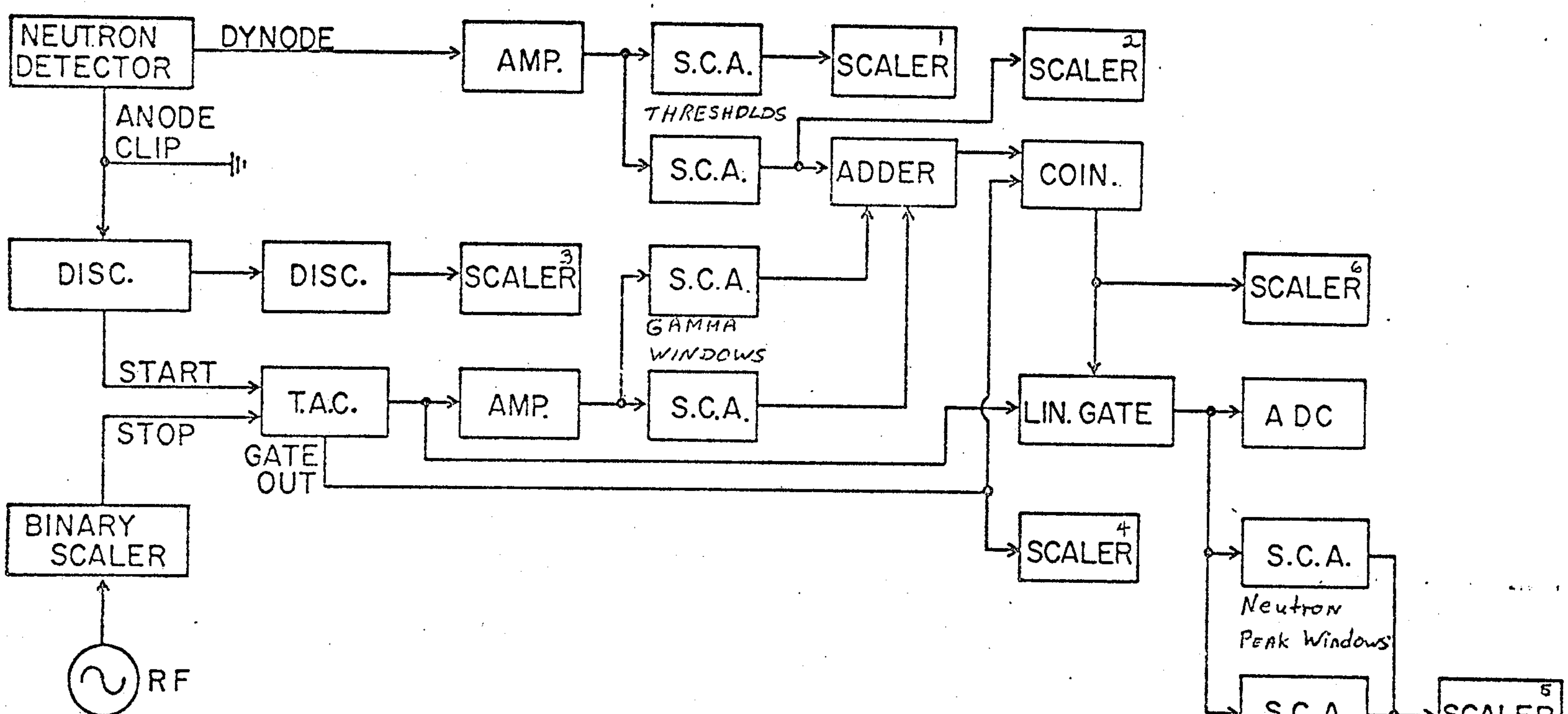
NEUTRON DETECTOR
DYNODE
ANODE CLIP
AMP.
S.C.A.
SCALER 1
SCALER 2
THRESHOLDS
S.C.A.
ADDER
COIN.
DISC.
DISC.
SCALER 3
S.C.A.
GAMMA WINDOWS
SCALER 6
START
STOP
T.A.C.
GATE OUT
AMP.
S.C.A.
LIN. GATE
A DC
BINARY SCALER
SCALER 4
S.C.A.
Neutron Peak Windows
S.C.A.
SCALER 5
RF

Figure (5)

A SAMPLE TIME OF FLIGHT SPECTRUM

This spectrum is a typical time of flight spectrum after all gating has been done. The prompt gamma peaks are riding on the background and have been gated into the otherwise gamma-free spectrum. Notice that to the right of the neutron peaks there is no measureable background at all. The structure to the left of the neutron peak is the characteristic low energy tail of neutrons from lithium.

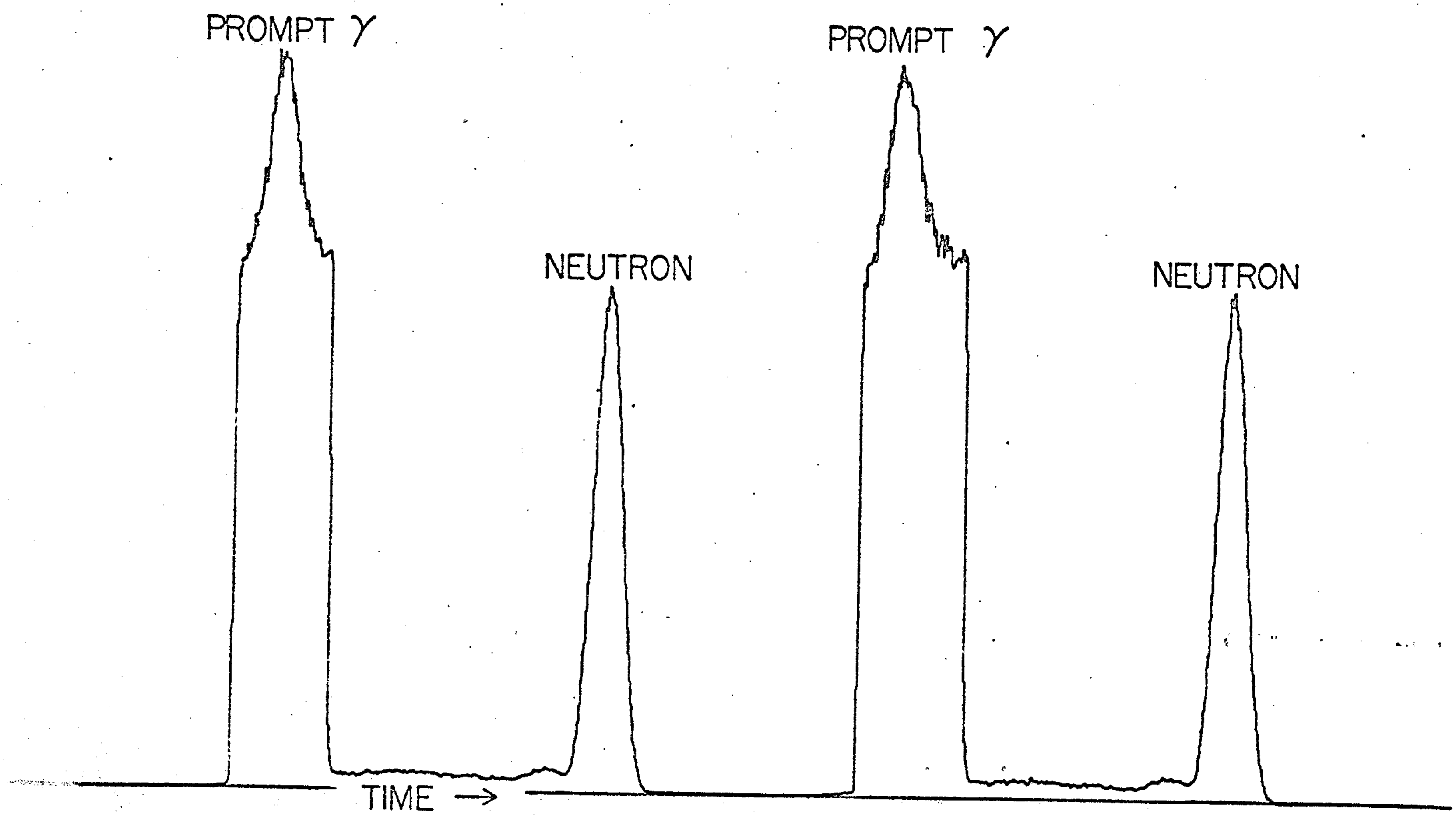
PROMPT γ
NEUTRON
PROMPT γ
NEUTRON
TIME →

2.3 EXPERIMENTAL PROCEDURE

The absorbers were changed approximately every 200 seconds to try to minimize the effect of changes in the photomultiplier gain, drifts in machine output, etc., during the period that the various absorbers were in place. Thus, every 200 seconds the computer stopped the scalers, the scaler readings were recorded, absorbers were changed and data was taken again in another region of the computer memory. A separate region was kept for each absorber. The abosrbers were rotated in the order: toluene, carbon, blank, carbon, toluene. After several cycles, the stored data was put onto magnetic tape to minimize data loss in the event of an operator mistake. Data was collected in this manner until the desired statistical accuracy was obtained.

A close watch was kept on the scaler readings and the position of the windows around the neutron peaks. In the event of a shift in phase of beam pulse relative to the r.f., the windows would have had to be reset. In fact, this was seldom necessary. Because the scaler readings were checked carefully, malfunctions were noticed quickly and could be corrected with a minimum of time loss.

3.1 CALCULATION OF CROSS SECTIONS

Because of the geometry of this experiment, any neutrons that were scattered in the absorbers would not be detected. For this reason, the neutron interaction is an all or nothing process in that if it reacts at all with the absorber nuclei it leaves the beam. In this way it is quite different to a charged particle which has its energy degraded while passing through the electron clouds of a substance. As a result, the attenuation takes the form:

$$\frac{N_1}{N_o} = \exp -n\sigma t \qquad \ldots (1)$$

Here, N_1 is the number passing through the material, N_o is the number incident, n is the number of atoms per unit volume, t is the thickness and σ is the total cross section.

Solving for the cross section:

$$\sigma = \frac{1}{nt} \ln \frac{N_o}{N_1} \qquad \ldots (2)$$

In this experiment, the values of N_1 and N_o were determined from the number of neutrons in the neutron peaks. The numbers were then normalized to the unattenuated neutron flux and corrected for dead time in the electronics. The quantity actually determined in the experiment was the attenuation factor, R.

i.e.

$$R = \frac{N_o}{N_1} \qquad \ldots (3)$$

As described earlier (page 3) toluene was used as the hydrogen absorber and a block of graphite was used to subtract the carbon in the toluene. In making the subtraction, the number of carbon atoms was not balanced exactly. As a result, we had to include a further subtraction in our calculation of the proton cross section. The attenuation R is composed of an attenuation due to hydrogen, R_p , plus an attenuation due to the unbalanced carbon, R_c.

Then $$R = R_p \cdot R_c$$

and $$\ln R = \ln R_p + \ln R_c$$

Substitute from the defining equations (2) and (3) to obtain:

$$\ln R = n_p t \sigma_p + n_c t \sigma_c \qquad \ldots (4)$$

where subscripts p and c refer to protons and carbon respectively, and cross sections are normalized.

Therefore: $$\sigma_p = \frac{1}{n_p t} (\ln R - n_c t \sigma_c) \qquad \ldots (5)$$

Here n_c is positive since there was an excess of carbon in the toluene. If there had been a deficiency of carbon in the toluene, the value n_c would be negative.

3.2 DETERMINATION OF ERRORS

To determine the uncertainty in the value of σ_p derived in equation (5), we write it in two parts:

$$\sigma_p = \frac{\ln R}{n_p t} - \frac{n_c t}{n_p t}\sigma_c = A + B \qquad \text{... (6)}$$

Then, adding in quadrature,

$$\Delta\sigma_p = \left[(\Delta A)^2 + (\Delta B)^2\right]^{\frac{1}{2}} \qquad \text{... (7)}$$

To find the individual parts, (ΔA) and (ΔB) , the standard method is used. The first part becomes:

$$\frac{(\Delta A)^2}{A^2} = \left[\frac{\Delta \ln R}{\ln R}\right]^2 + \left[\frac{\Delta n_p t}{n_p t}\right]^2 = \left[\frac{\Delta R}{R \ln R}\right]^2 + \left[\frac{\Delta n_p t}{n_p t}\right]^2 \qquad \text{... (8a)}$$

and similarly the second term is:

$$\frac{(\Delta B)^2}{B^2} = \left[\frac{\Delta n_c t}{n_c t}\right]^2 + \left[\frac{\Delta \sigma_c}{\sigma_c}\right]^2 + \left[\frac{\Delta (n_p t)}{n_p t}\right]^2 \qquad \text{... (8b)}$$

Since A and B are known, equation 7 will give a standard error or uncertainty.

An idea of the typical size of the various terms in these error equations is given by the example in Table I. Here, the 37.11 MeV measurement has been used as a typical example.

TABLE I

Term	Size	Term	Size
$\frac{\Delta \ln R}{\ln R}$	.012	$\frac{\Delta \sigma_c}{\sigma_c}$	.020
$\frac{\Delta n_p t}{n_p t}$	.005	$\frac{\Delta n_c t}{n_c t}$	.005
ΔA	.0038	ΔB	.0013
$\frac{\Delta \sigma_p}{\sigma_p}$	.0151		

3.3 DETERMINATION OF THE ATTENUATION AND ITS STATISTICAL UNCERTAINTY

The attenuation factor R must be normalized and corrected for dead time. Normalization is accomplished by dividing the number of peak neutrons by the number of monitor counts in the same period of time.

However, this is still not an accurate representation of the number of neutrons since some neutron pulses from the detector were lost during the time the TAC was inactive. This can be corrected since we know the number of pulses that were seen at the start of the TAC and the number of pulses the TAC had analysed. By multiplying the number of neutrons by the ratio of the TAC start pulses to TAC analysed pulses, we correct for the percentage of pulses lost at the TAC. The final neutron intensity is given by:

$$N = \frac{I}{M} \cdot \frac{T_s}{T_g}$$

where I is the number of peak neutrons,

M is the number of monitor neutrons,

T_s is the number of TAC start pulses, and

T_g is the number of TAC pulses analysed.

This must be calculated for both N_o and N_1 in equation (2). Hence the attenuation factor is:

$$R = \frac{N_o}{N_1}$$

where N_o and N_1 are calculated in the above way.

The uncertainty in the attenuation factor comes from the statistical uncertainty in each of the eight numbers involved in its calculation.

i.e.

$$\frac{\Delta R}{R} = \left[\left(\frac{\Delta I_o}{I_o}\right)^2 + \left(\frac{\Delta M_o}{M_o}\right)^2 \text{........ etc.}\right]^{\frac{1}{2}}$$

For statistical values,

$$\frac{\Delta I_o}{I_o} = \frac{1}{I_o^{\frac{1}{2}}}$$

So the uncertainty in the attenuation factor is:

$$\frac{\Delta R}{R} \quad \left[\frac{1}{I_o} + \frac{1}{M_o} + \frac{1}{T_{so}} + \ldots \text{ etc.}\right]^{\frac{1}{2}}$$

Again, eight numbers are involved. These are peak neutrons, normalization, TAC starts, and TAC output pulses for both absorbers.

About two-thirds of the uncertainty in the cross section is from statistics, with the rest coming from density measurements and uncertainty in carbon cross sections.

3.4 INTERNAL CONSISTENCY

The absorbers were moved in and out of the beam with each absorber spending 200 seconds in the beam. For each 200 second carbon and toluene pair, a cross section can be calculated, although the statistical uncertainty may be quite large. As many as twenty of these may be required for the final high precision data. A check of the internal consistency of the results can then be made. The standard error in the mean can be calculated in two ways. One way is to determine it from the deviation between the individual cross sections and the mean. This gives an error:

$$\alpha_e = \left[\frac{\sum_s (\sigma_s - \bar{\sigma})^2 w_s}{(n-1) \sum_s w_s} \right]^{\frac{1}{2}}$$

where w_s is the weight of cross section σ_s in the calculation of the average, $\bar{\sigma}$. The value n is the number of cross sections σ_s involved.

The other method of determining the standard error in the mean is from the statistical uncertainties of the individual cross sections. If the statistical uncertainty for cross section σ_s is α_s , the error in the mean is:

$$\alpha_i = \frac{(\sum_s w_s{}^2 \alpha_s{}^2)^{\frac{1}{2}}}{\sum_s w_s}$$

For the statistical case, w_s is proportional to $1/\alpha_s^2$. The ratio of α_e to α_i then becomes a consistency ratio and has the form:

$$\frac{\alpha_e}{\alpha_i} = \left[\frac{\sum_{s=1}^{n} (\sigma_s - \bar{\sigma})/\alpha_s^2}{(n-1)}\right]^{\frac{1}{2}}$$

This ratio should be nearly unity and the uncertainty or expected deviation from one is:

$$\Delta = \pm \frac{1}{2(n-1)^{1/2}}$$

These ratios were calculated for all data used and were found to be unity within the expected tolerances. This indicates that the consistency in the results is as good as the statistics, which is in the order of 0.3 percent for most of the points.

In Table III the full set of σ_s and α_s values used in the final data is given. Also included is the mean $\bar{\sigma}$ and the value of α_e/α_i with its expected deviation from unity. Note that the values of and σ_s are not complete in that density and thicknessare not included in their calculation.

i.e. $\sigma_s = \ln R_s$ and

$\bar{\sigma} = \ln \bar{R}$

The value SIGMA in Table II is σ_s and is unitless and the ERROR is due to statistics alone. The values for peak neutrons, monitor neutrons, etc. are summed values which were used in calculation of $\bar{\sigma}$ which is given as average sigma in the table. The consistency ratio α_e/α_i is also given with its expected deviation from unity, i.e. Δ.

TABLE II

ENERGY: 25.60 MeV

Sigma	Error	Sigma	Error
0.543083	0.0212745	0.583277	0.0210803
0.565358	0.0212518	0.564103	0.0210050
0.531071	0.0206753	0.547897	0.0207899
0.565564	0.0212887	0.589792	0.0215038
0.522041	0.0207482	0.560408	0.0187712
0.593155	0.0188919	0.550804	0.0172372
0.548901	0.0191366	0.527253	0.0192372
0.578143	0.0196813	0.562510	0.0177845
0.501955	0.0199345	0.000000	0.0000000

	Peak Neutrons	Monitor Neutrons	TAC Starts	TAC Stops
Carbon Absorber	145260.	1834659.	1948308.	1942065.
Toluene Absorber	84895.	1864559.	821179.	819998.

Average Sigma is 0.555045

Statistical Error is 0.0048177

The Consistency Ratio (P.27) is 1.2356

Allowed Deviation from 1.0 is 0.1768

TABLE II cont'd.

ENERGY: 26.87 MeV

Sigma	Error	Sigma	Error
0.518073	0.0224877	0.511274	0.0219259
0.474557	0.0191913	0.542197	0.0193338
0.491927	0.0190727	0.541982	0.0188821
0.503663	0.0188353	0.514951	0.0187378
0.569640	0.0185334	0.525198	0.0185288
0.521990	0.0187492	0.533244	0.0189907
0.532734	0.0185068	0.516554	0.0183193
0.522084	0.0184045	0.535140	0.182985
0.529482	0.0185157	0.523291	0.0225523
0.534333	0.0221036	0.509723	0.0203979

	Peak Neutrons	Monitor Neutrons	TAC Starts	TAC Stops
Carbon Absorber	162547.	3314449.	3827671.	3808149.
Toluene Absorber	96147.	3298135.	1860186.	1855293.

Average Sigma is 0.522633

Statistical Error is 0.0043311

The Consistency Ratio (P.27) is 1.0486

Allowed Deviation from 1.0 is 0.1622

TABLE II cont'd.

ENERGY: 26.90 MeV

Sigma	Error	Sigma	Error
0.534804	0.0111081	0.547138	0.0111670
0.519740	0.0111311	0.527244	0.0102576
0.522388	0.0102085	0.538958	0.0104070
0.542641	0.0103613	0.000000	0.0000000

	Peak Neutrons	Monitor Neutrons	TAC Starts	TAC Stops
Carbon Absorber	207866.	757336.	11205060.	10821830.
Toluene Absorber	121601.	745676.	6970072.	6816759.

Average Sigma is 0.533189

Statistical Error is 0.0040209

The Consistency Ratio (P.27) is 0.9692

Allowed Deviation from 1.0 is 0.2887

TABLE II cont'd.

ENERGY: 30.40 MeV

Sigma	Error	Sigma	Error
0.474243	0.0113805	0.470803	0.0113281
0.463709	0.0112755	0.489235	0.0112702
0.461361	0.0112272	0.482180	0.0111270
0.492276	0.0113065	0.473185	0.0113062
0.454876	0.0113517	0.463201	0.0113267
0.456242	0.0113092	0.464965	0.0114444
0.493169	0.0114948	0.000000	0.0000000

	Peak Neutrons	Monitor Neutrons	TAC Starts	TAC Stops
Carbon Absorber	345280.	1241388.	8158946.	8041630.
Toluene Absorber	215931.	1237090.	4444158.	4407907.

Average Sigma is 0.472220

Statistical Error is 0.0031369

The Consistency Ratio (P.27) is 1.1717

Allowed Deviation from 1.0 is 0.2041

TABLE II cont'd.

ENERGY: 31.96 MeV

Sigma	Error	Sigma	Error
0.443867	0.0140468	0.413896	0.0140737
0.446976	0.0140085	0.423877	0.0182756
0.388870	0.0184838	0.466557	0.0183406
0.464431	0.0156010	0.470974	0.0157836
0.444998	0.0159452	0.422900	0.0200819
0.434854	0.0154696	0.000000	0.0000000

	Peak Neutrons	Monitor Neutrons	TAC Starts	TAC Stops
Carbon Absorber	161117.	613466.	2198948.	2186902.
Toluene Absorber	105154.	625938.	1132970.	1129885.

Average Sigma is 0.449596

Statistical Error is 0.0046501

The Consistency Ratio (P.27) is 1.6051

Allowed Deviation from 1.0 is 0.2236

TABLE II cont'd.

ENERGY: 33.96 MeV

Sigma	Error	Sigma	Error
0.366757	0.195487	0.390393	0.0191544
0.408525	0.0197279	0.419746	0.0195406
0.376174	0.0195572	0.392945	0.0168280
0.391640	0.0167438	0.378514	0.0167393
0.422407	0.0164761	0.406815	0.0165646
0.385054	0.0164345	0.394862	0.0160683
0.503227	0.0173033	0.374012	0.0170559
0.447903	0.0160494	0.431178	0.0149488
0.430173	0.0152282	0.396017	0.0151593
0.401813	0.0150328	0.000000	0.0000000

	Peak Neutrons	Monitor Neutrons	TAC Starts	TAC Stops
Carbon Absorber	190517.	1939904.	5613634.	5565251.
Toluene Absorber	130640.	1992609.	3210606.	3195723.

Average Sigma is 0.408111

Statistical Error is 0.0038604

The Consistency Ratio (P.27) is 1.8607

Allowed Deviation from 1.0 is 0.1667

TABLE II cont'd.

ENERGY: 34.45 MeV

Sigma	Error	Sigma	Error
0.430281	0.0221970	0.435671	0.0222826
0.470521	0.0223179	0.389356	0.0225680
0.406073	0.0168783	0.424749	0.0172942
0.435395	0.0171740	0.461493	0.0185187
0.417276	0.0172770	0.418576	0.0176972

	Peak Neutrons	Monitor Neutrons	TAC Starts	TAC Stops
Carbon Absorber:	154667.	120649.	5222432.	5158844.
Toluene Absorber:	100837.	118952.	3025542.	3003487.

Average Sigma is 0.418537

Statistical Error is 0.0058418

The Consistency Ratio (P.27) is 1.2907

Allowed Deviation from 1.0 is 0.2357

TABLE II cont'd.

ENERGY: 37.11 MeV

Sigma	Error	Sigma	Error
0.355102	0.0197983	0.364571	0.0197276
0.352930	0.0186381	0.369589	0.0185359
0.343699	0.0186625	0.384703	0.0189887
0.341625	0.0190542	0.364711	0.0194292
0.385131	0.0192984	0.347337	0.0192105
0.363064	0.0191390	0.357772	0.0186636
0.366482	0.0193877	0.371344	0.0186409
0.333571	0.0186839	0.339852	0.0189624
0.394185	0.0189139	0.371656	0.0187340

	Peak Neutrons	Monitor Neutrons	TAC Starts	TAC Stops
Carbon Absorber	139392.	1352066.	5027621.	4990674.
Toluene Absorber	96740.	1342633.	2937776.	2925139.

Average Sigma is 0.361325

Statistical Error is 0.0044807

The Consistency Ratio (P.27) is 0.8846

Allowed Deviation from 1.0 is 0.1715

TABLE II cont'd.

ENERGY: 37.87 MeV

Sigma	Error	Sigma	Error
0.372129	0.0231462	0.449574	0.0232310
0.399137	0.0228660	0.361912	0.0229281
0.367728	0.0232905	0.385081	0.0237533
0.352117	0.0251577	0.385641	0.0283211
0.350943	0.0249917	0.357882	0.0262692
0.306756	0.0270583	0.282097	0.0270827
0.378632	0.0277096	0.000000	0.0000000

	Peak Neutrons	Monitor Neutrons	TAC Starts	TAC Stops
Carbon Absorber:	105888.	88681.	3631114.	3605255.
Toluene Absorber:	73018.	88278.	2050072.	2041388.

Average Sigma is 0.370022

Statistical Error is 0.0068756

The Consistency Ratio (P.27) is 1.6228

Allowed Deviation from 1.0 is 0.2041

TABLE II cont'd.

ENERGY: 42.81 MeV

Sigma	Error	Sigma	Error
0.257363	0.0235440	0.339837	0.0222362
0.302830	0.0206018	0.295452	0.0192502
0.369582	0.0196194	0.333758	0.0158782
0.319651	0.0157997	0.343228	0.0159381
0.268558	0.0161147	0.276104	0.0160793
0.312380	0.0161307	0.287877	0.0156873
0.334495	0.0162119	0.287400	0.0162869
0.320972	0.0170549	0.335213	0.0170642

	Peak Neutrons	Monitor Neutrons	TAC Starts	TAC Stops
Carbon Absorber	156176.	1143103.	3390885.	3369675.
Toluene Absorber	113750.	1131408.	1931425.	1923665.

Average Sigma is 0.308944

Statistical Error is 0.0043107

The Consistency Ratio (P.27) is 1.7085

Allowed Deviation from 1.0 is 0.1826

3.5 ENERGY DETERMINATION

The energy of the neutrons in the peak is determined by measuring their time of flight over a known 500 cm. path. This gives the velocity which is put into the relativistic equation for the kinetic energy.

To determine the flight time, two things are needed. We need first to know when the flight started. This is determined from the arrival time of the prompt γ rays that left the lithium at the same time as the neutrons. We know these γ rays took 16.7 nsec. to reach the detector.

$$t_\gamma = \frac{500 \text{ cm.}}{29.98 \text{ cm/nsec.}} = 16.7 \text{ nsec.}$$

Thus we can find the starting time.

Secondly, we must know how many r.f. periods (about 35.11 nsec. each) the neutron is delayed with respect to the gamma ray before it is detected. This is necessary since our time spectrum is really made up of two r.f. periods so that 35.11 nsec. is the longest time we can directly measure. Thus to get the correct neutron flight time, the number of r.f. periods must be added to the time measured directly on the time spectrum. A diagram showing the position in space of succesive bursts of gamma and neutron pulses is given in figure (6).

Once the velocity of the neutrons is determined, the kinetic energy can be found by substituting into the relativistic equation,

$$E_K = E_T - E_0 = m_0c^2 \left[\frac{1}{(1-(v/c)^2)^{1/2}} - 1 \right]$$

In this equation E_K is the neutron kinetic energy,

E_0 is the rest mass energy,

E_T is the total neutron energy,

m_0 is the neutron rest mass, and

v is the neutron velocity.

As an example, for the case shown in figure (6), the neutron velocity is 8.48 cm/nsec. This gives a value of 977.9 MeV for the total energy which leaves about 40 MeV of kinetic energy for a neutron rest mass of 938 MeV.

Figure (6)

RELATIVE POSITIONS OF γ AND n PULSES

Figure (6a) shows the position in space of the neutron and gamma pulses at the moment a gamma is detected at the five metre mark. Dashed lines show which gamma corresponds to which neutron. Note that when the n^{th} gamma is detected, the $(n-1)^{th}$ neutron is 7.1 nsec. away from the detector.

Figure (6b) is a sketch of the resulting time spectrum. There is a 7.1 nsec. separation between the neutron and the prompt gamma. This corresponds to a total flight time of 58.9 nsec. which would be the value used to calculate the energy.

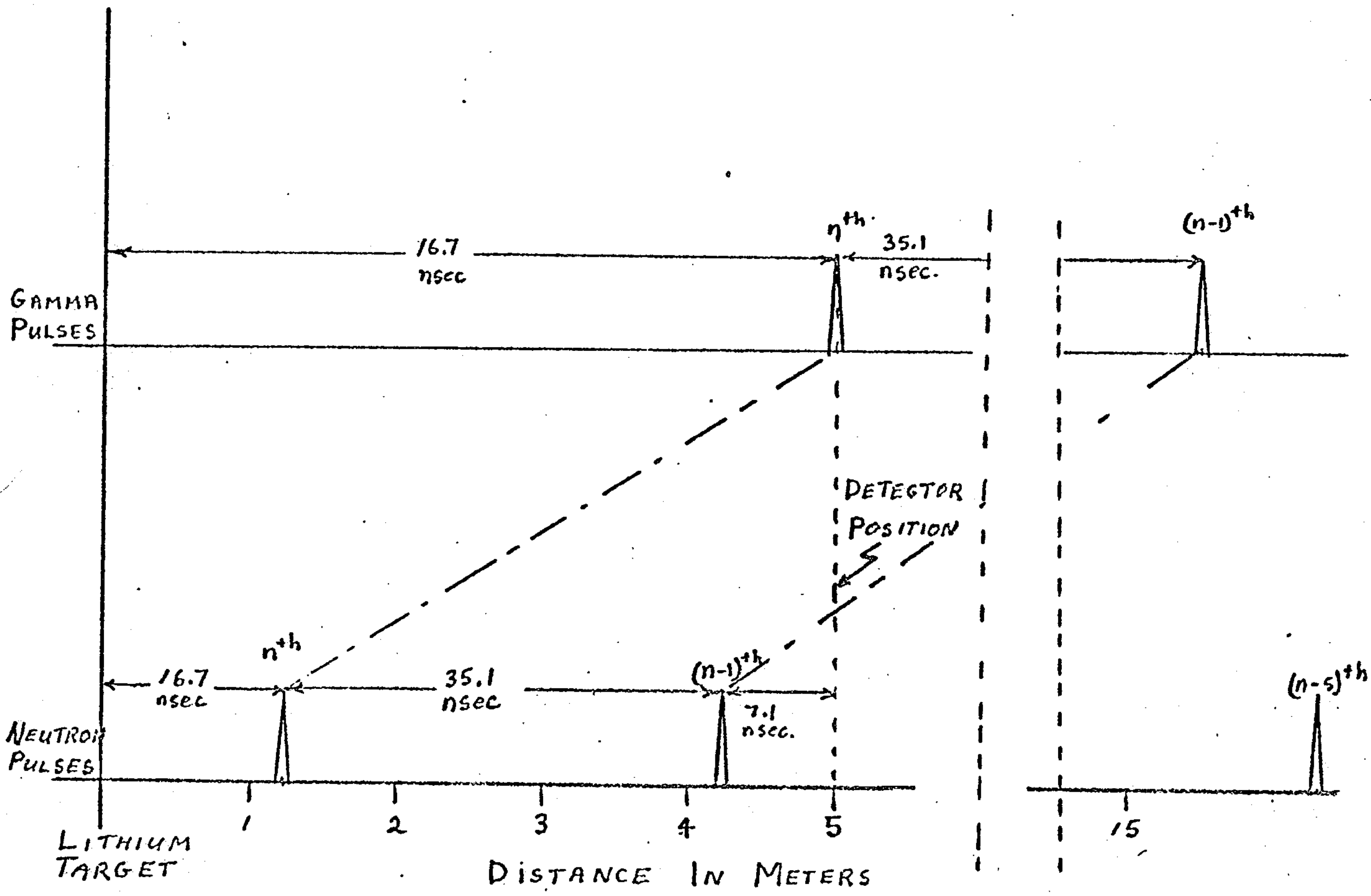
16.7
nsec
n^{th}
35.1
nsec.
$(n-1)^{th}$
Gamma
Pulses
Detector
Position
n^{th}
16.7
nsec
35.1
nsec
$(n-1)^{th}$
7.1
nsec.
$(n-5)^{th}$
Neutron
Pulses
1
2
3
4
5
15
Lithium
Target
Distance In Meters

fig. 6a

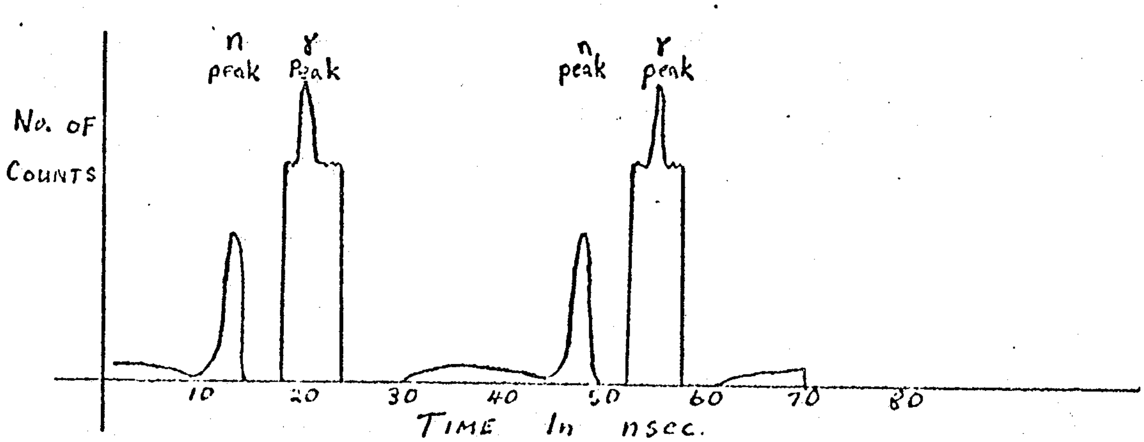
n
peak
γ
Peak
n
peak
γ
peak
No. of
Counts
10
20
30
40
50
60
70
80
Time In nsec.

fig. 6b

L EXPERIMENTAL RESULTS

The data which spans the energy range from twenty-five to forty-three MeV was compared to the already-published data and is shown plotted in figure (7). The actual data as measured is given in Table III. Cross sections for the carbon were obtained from published results.

The curve shown by the solid line is a smooth curve through the points at 20, 25, 30, 40, and 50 MeV given by the MacGregor phase shift tables. The plotted points on the average are 3 to 5 millibarns higher than this curve. Calculations for the curve are given in Appendix C.

Agreement of results measured in this experiment with those published by U.C. Davis in this energy range appears to be good within about 1.5% and the overall agreement among data from U.C. Davis, Canberra, Wisconsin (9) and Manitoba between 25 and 28 MeV is excellent.

There are two conclusions that arise from the data presented in figure (7). The first is that the n-p cross section may now be considered as well determined in this energy range to an accuracy of 1.5% or better. The agreement between the various published values and our own measurements is within the errors quoted.

The second result is the fact that the measured values are higher than the phase shift derived cross sections. While this difference amounts to only about 1.5%, it is consistent in that only one measured point is below the curve. On the other hand, fifteen are clearly above it and three have error bars that overlap it. The conclusion would be that the curve is low by about one to one and a half percent.

TABLE III

ENERGY (MeV)	CROSS SECTION (Millibarns)	ENERGY (MeV)	CROSS SECTION (Millibarns)
25.60	374.1 ± 3.9	33.96	269.5 ± 3.2
26.87	352.3 ± 3.6	34.45	265.5 ± 4.6
26.90	347.3 ± 3.4	37.11	236.6 ± 3.6
30.40	303.0 ± 2.8	37.87	223.1 ± 5.3
31.96	291.0 ± 3.6	42.81	199.7 ± 3.4

Figure (7)

PLOT OF DATA

Data is shown plotted on a log-log graph. Note that the measured points are consistantly above the curve.

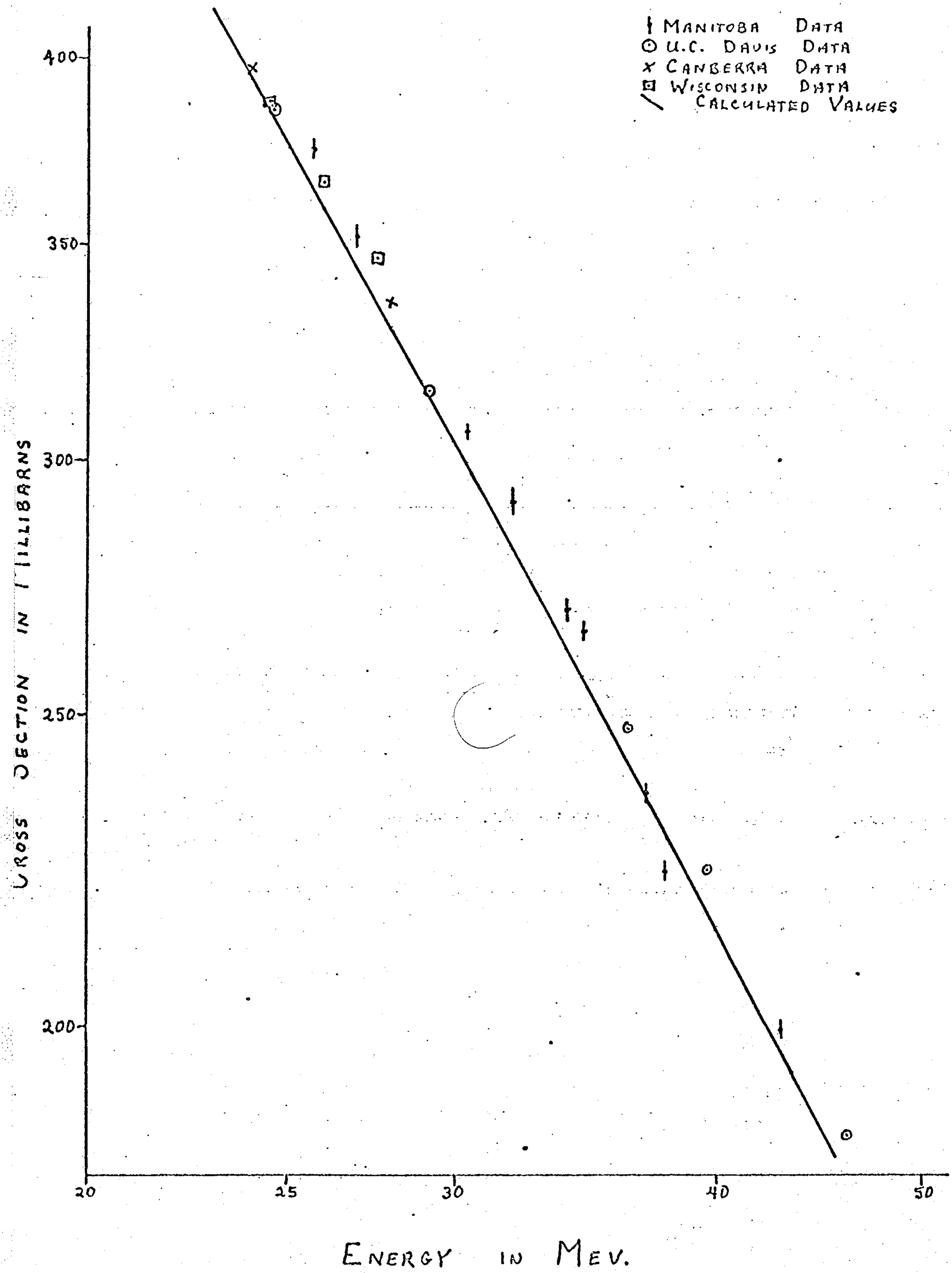

Manitoba Data
U.C. Davis Data
Canberra Data
Wisconsin Data
Calculated Values
400
350
300
250
200
Cross Section in Millibarns
20
25
30
40
50
Energy in Mev.

Fig. 7

REFERENCES

1) Gy. Hreuss and T. Czibok, Phys. Letters 28B 585 (1969)

2) H.P. Noyes, Phys. Rev. 130 2025 (1963)

3) S. Cierjacks, P. Forti, G.J. Kirouac, D. Kopsch, L. Dropp, and J. Nebe, Phys. Rev. Letters 23 866 (1969)

4) M.H. MacGregor, R.A. Arndt, and R.M. Wright, Phys. Rev. 182 1714 (1969)

5) P.H. Bowen, J.P. Scanlon, G.A. Stafford, and J.J. Thresher, Nucl. Phys. 22 640 (1961)

6) F.P. Brady, W.J. Knox, J.A. Jungerman, M.R. McGie, and R.L. Walraven, Phys. Rev. Letters 25 1628 (1970)

7) O.E. Groce, B.D. Sowerby, Nucl. Phys. 83 199 (1966)

8) J.L. Gammel, Fast Neutron Physics
John Wiley and Sons, New York - London p.2183 (1963)

9) J.C. Davis and H.H. Barschall, Phys. Rev. 3 1798 (1971)

10) J. Topping, Errors of Observation and Their Treatment
Chapman & Hall Ltd., London p.91 (1965)

APPENDIX A

FURTHER EXPLANATION OF FIGURE (7)

Since figure (7) is a log-log plot and one may want to read data off it or plot further data on it, the following equations for the x and y co-ordinates are given.

$$x = 37.67 \log_{10} E - 49.1$$

$$y = 57.67 \log_{10} \sigma_T - 130.07$$

where x,y are in centimeters,

E is energy in MeV, and

σ_T is cross section in millibarns.

The y-axis goes from 180 mb. at $y = 0$ to 400 mb. at $y = 20$cm. The x-axis is 20 MeV at $x = 0$ and 50 MeV at $x = 15$cm.

APPENDIX B

The following two pages contain the schematic diagrams for the timing base used for the 8575 and for the dynode preamplifier.

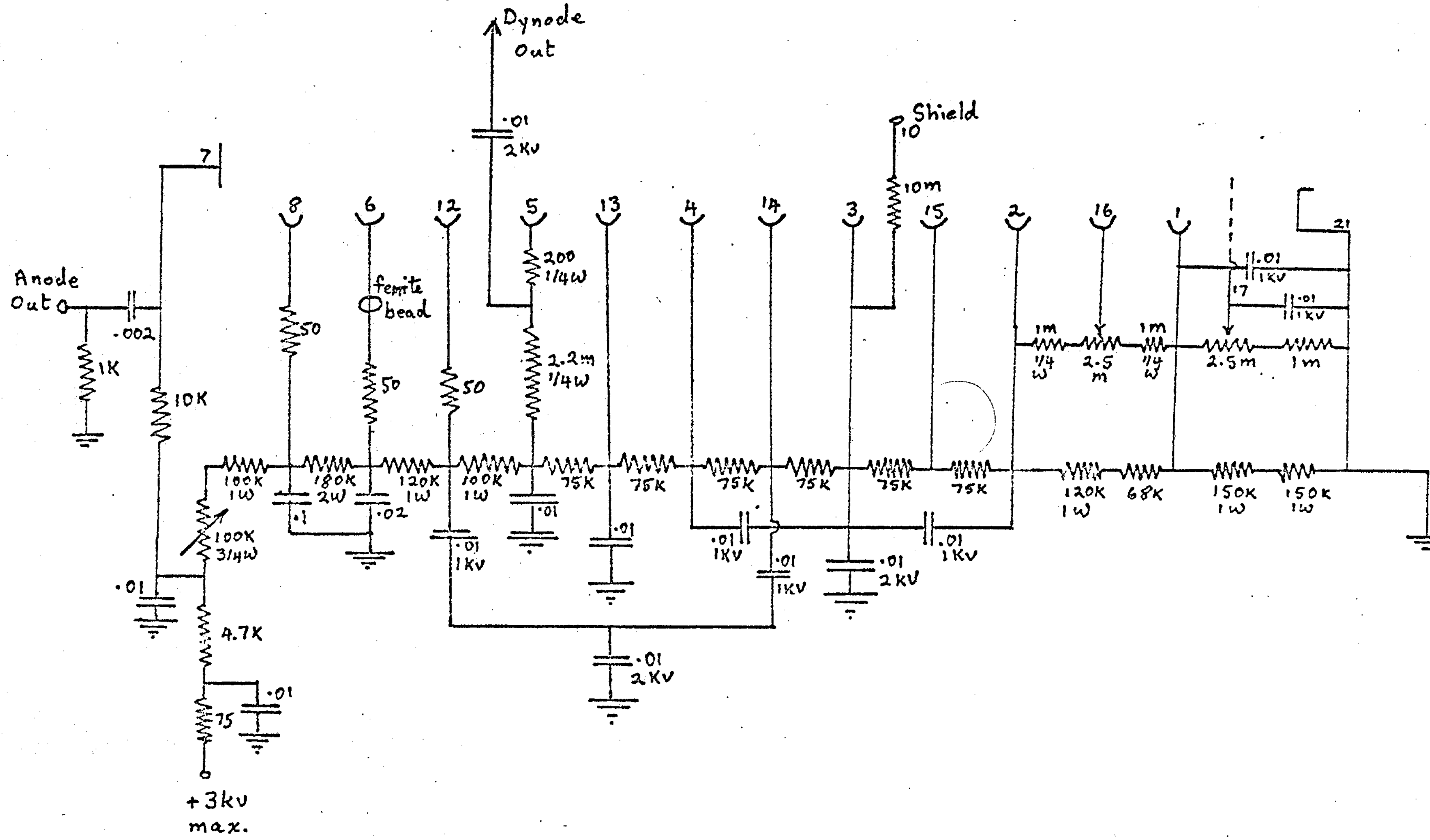

All resistors ½w 5%, all capacitors are 3kv unless otherwise noted.

RCA 8575 Base Diagram

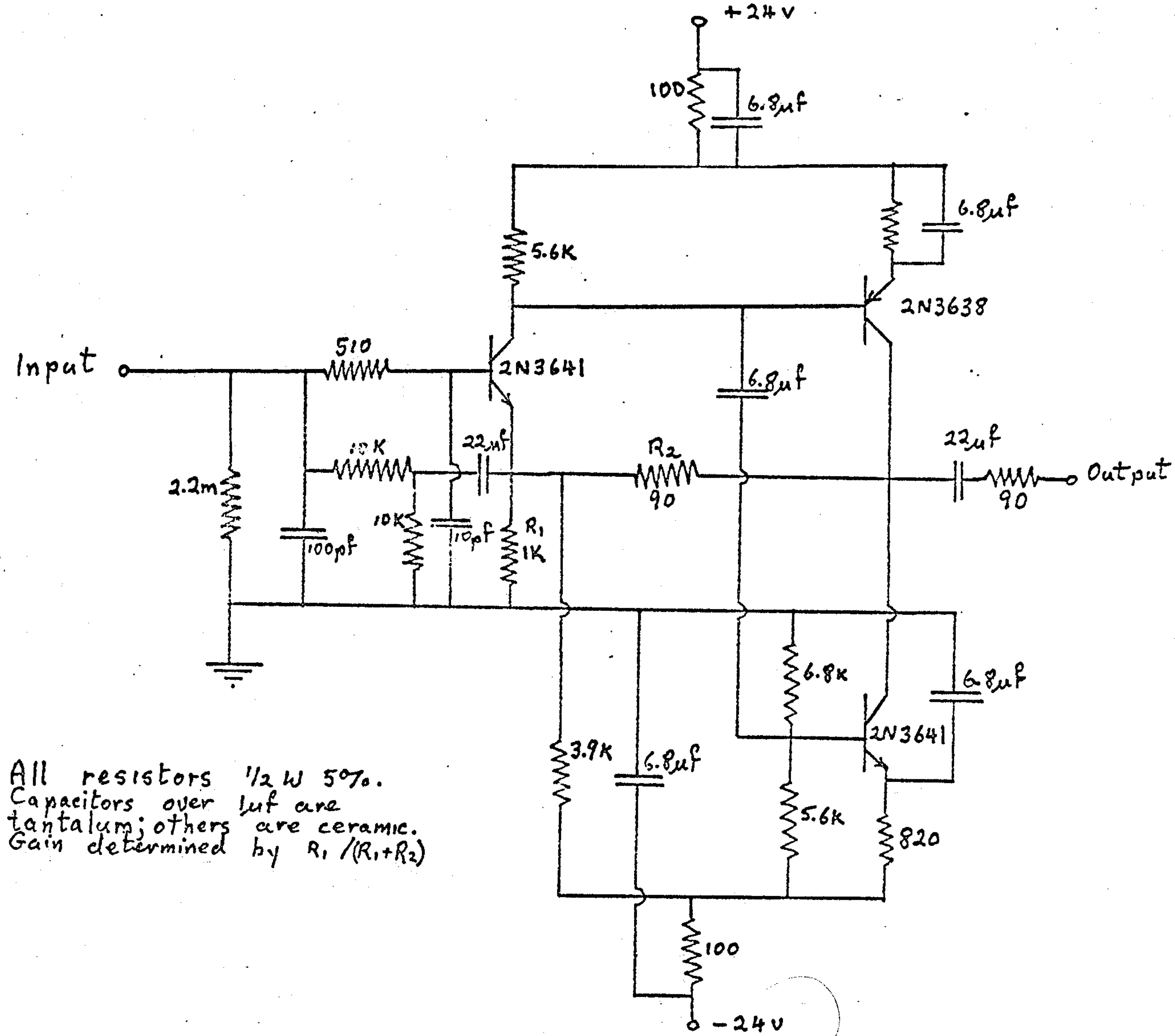

All resistors 1/2 W 5%.
Capacitors over 1µf are tantalum; others are ceramic.
Gain determined by $R_1/(R_1+R_2)$

Dynode Preamplifier

APPENDIX C

The total cross section was calculated from the phase shifts by the following method. The cross section is given by:

$$\sigma_{np} = \frac{8\pi}{k} \, Im\,(\alpha_{np})$$

where k is in the centre of mass frame. The values for α_{np} are given by:

$$\alpha_{np} = \frac{1}{4} \left\{ 2\, f_{1,1} + f_{o,o} + f_{s,s} \right\}$$

where the f_{ij} are scattering amplitudes for zero degrees.

i.e. $f_{s,s}$ is the singlet amplitude

$f_{1,1}$ is the triplet for paired spins (↑↑ or ↓↓)

and $f_{o,o}$ is the triplet for opposite spins (↑↓).

These were determined by summing over l values the various phase shifts with their appropriate amplitudes. The phase shifts δ and the coupling ratios ε used in the summations were listed in the paper by MacGregor.